We are IntechOpen, the world's leading publisher of Open Access books
Built by scientists, for scientists

6,900
Open access books available

185,000
International authors and editors

200M
Downloads

154
Countries delivered to

Our authors are among the

TOP 1%
most cited scientists

12.2%
Contributors from top 500 universities

WEB OF SCIENCE™

Selection of our books indexed in the Book Citation Index
in Web of Science™ Core Collection (BKCI)

Interested in publishing with us?
Contact book.department@intechopen.com

Design of Cooling Units for Heat Treatment

Michal Pohanka and Petr Kotrbáček

Additional information is available at the end of the chapter

1. Introduction

Microstructure and nature of grains, grain size and composition determine the overall mechanical behavior of steel. Heat treatment provides an efficient way to manipulate the properties of steel by controlling the cooling rate. The way of heat treatment depends on many aspects. One of the most important parameter is the amount of production. Another important parameter is the size of products. We focus here on large production such as interstand [1] and run-out table cooling of hot rolled strip, run-out table cooling of sheets and plates, cooling of long products at the exit from a rolling mill, cooling of rails, tubes and special profiles [2], continuous hardening and heat treatment lines for steel strips. Such a treatment is called in-line heat treatment of materials and has become frequently used by hot rolling plants. This method achieves the required material structure without the necessity of reheating. In-line heat treatment is characterized by running of hot material through the cooling section. However, many of discussed topics can be applied on smaller production as well.

The design procedure of cooling sections for obtaining the demanded structure and mechanical properties is iterative research involving several important steps. We begin with the Continuous Cooling Transformation (CCT) diagram for the selected material. Numerical simulation of cooling follows to find appropriate cooling intensity and its duration. Knowing the desired cooling intensity new cooling section is designed and tested under the laboratory conditions [3]. From the laboratory experiments boundary conditions are obtained and tested using a numerical model. When the best solution is found it is tested on the real sample and the result structure is studied. In most cases the process must be repeated as the CCT diagram is aimed at a different size of the sample and the cooling rate in the designed section is not constant.

2. Strategy of design

When preparing a design of the cooling system for the continuous heat treatment, we should know the optimum cooling regime for the material and the product. Any continuous heat treatment process needs to vary the cooling intensity with time. Moreover, the practice has shown that the results obtained by using small samples (usually for the CCT diagram) are usually different from the results achieved when using real products of a large cross-section because it is not possible to achieve the identical temperature regimes in the whole volume due to the low diffusivity. We cannot expect same behavior on product as on the small sample.

Next considerations focus on technical means that can be used to achieve the demanded temperature mode. There are varieties of technical methods for hot steel cooling; one of them uses the spray cooling. The cooling section should ensure reaching a required temperature history in the cooled piece prescribed by the metallurgists. The nozzles applied allow controlling the cooling over a wide range. The cooling intensity of groups of the nozzles must be measured and then the results obtained can be used in a numerical model of the temperature field in the cooled material.

2.1. Leidenfrost effect and its impact

It should be understand that intensity of cooling strongly depends on the surface temperature. So called Leidenfrost effect can be observed above certain temperature. During this effect a liquid, which is near significantly hotter object than the liquid's boiling point, produces vapor layer which insulates the liquid from the hot object and keeps out that liquid from rapid boiling. This is because of the fact that at temperatures above the Leidenfrost point, the part of the water, which is near hot surface, vaporizes immediately on contact with the hot plate and the generated gas keeps out the rest of the liquid water, preventing any further direct contact between the liquid water and the hot plate. The temperature at which the Leidenfrost effect begins to occur is not easy to predict. It depends on many aspects. Ones of them are velocity and size of droplets. As a rough estimate, the Leidenfrost point might occur for quite low temperatures such as 200 °C. On the other hand for high water velocity the Leidenfrost point can be even above 1000 °C. Fig. 1 shows measured heat transfer coefficients (HTC) for water-air mist nozzle. Graph shows three measurements for same nozzle using varying water and air parameters. Three regimes can be found. The first one is for low temperatures when the HTC is relatively high and decreasing slowly. This part is below Leidenfrost point. From certain temperature HTC decreases rapidly. This is a transient regime in which some droplets are above Leidenfrost point and some are below that point. For the last regime HTC is relatively low and is constant or may be increasing due to the increasing radiation with the increasing surface temperature. Designed cooling section should work in the first regime for low temperatures or in the third regime with almost constant HTC. It is strongly recommended to avoid the second transient regime as the product surface temperature is not usually at uniform temperature. Due to the strong dependency of HTC on surface temperature non homogeneous cooling is achieved and causes distortion of the product.
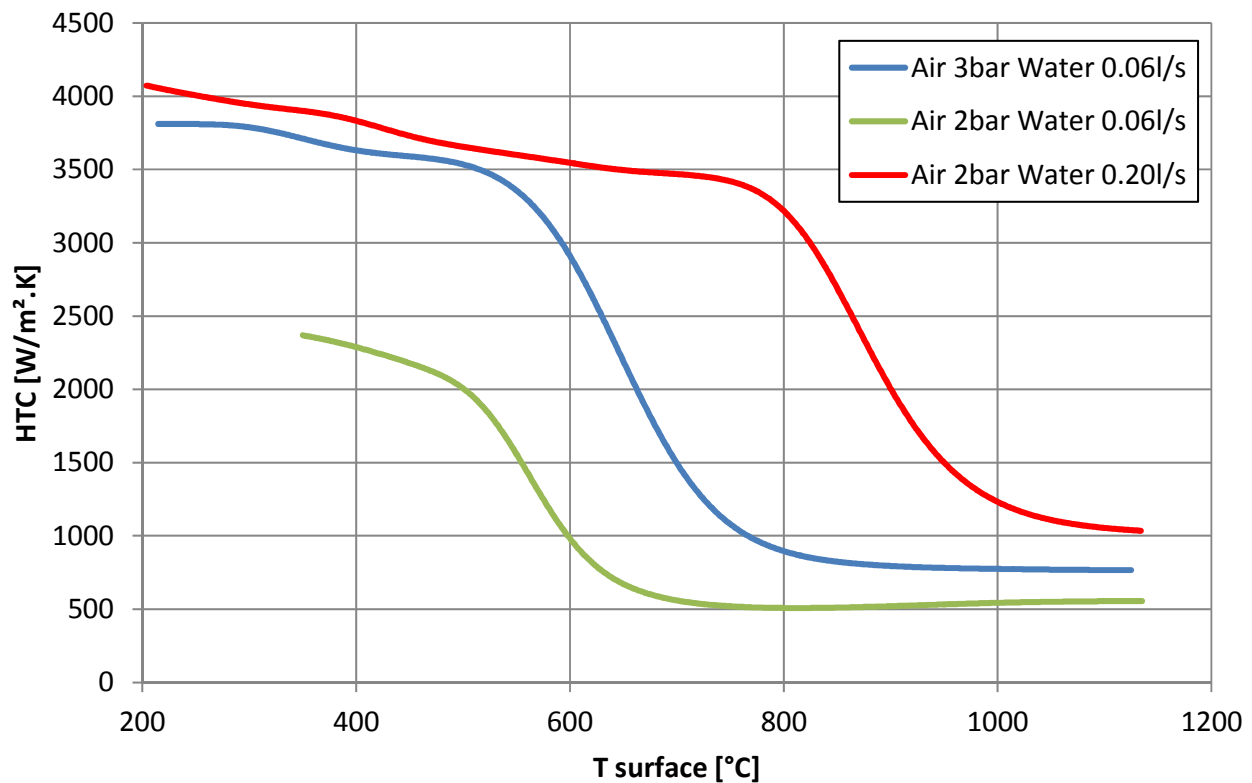
Figure 1. Moving Leidenfrost point for water-air mist nozzle and various water and air conditions.

2.2. Nozzle types and controllability

Nozzle produces usually one of three typical sprays: flat-jet, full-cone, and solid-jet (see Fig. 2). However, other shapes can be found such as hollow-cone, square, spiral etc. An important parameter is controllability of the cooling section and intensity of cooling. The water-air mist nozzles can be used for a soft cooling and a wide controllability range (see Fig. 3). The HTC can vary from several hundreds of W/m².K up to several thousand of W/m².K. Water-air mist nozzles are not the cheapest ones and also the pressurized air is expensive in terms of power consumption. Water-only nozzles can often provide a lower cost solution. Small full-cone nozzles with high pressure and bigger distance from surface can provide also very soft cooling. On the other hand with high pressure flat-jet or solid-jet nozzles at small distances HTC over 50000 W/m².K can be obtained even for high surface temperatures (see Fig. 4). This results in enormous heat flux above 50 MW/m². The distance of the nozzle form surface is very important in this case for flat-jet nozzles because for 100 mm the HTC can be 50000 W/m².K but for 1000 mm it can be similar to water-air mist nozzle. As conclusion we can say that for soft cooling air-mist or full-cone water only nozzles can be used and for hard cooling flat-jet nozzles with small distances are used. In some cases solid-jet nozzles are used for hard cooling but there are often two major problems: large amount of water generates a water layer on the product and the spray spot is small which causes non homogenous cooling. On the other hand, clogging is not big problem for solid-jet nozzles.
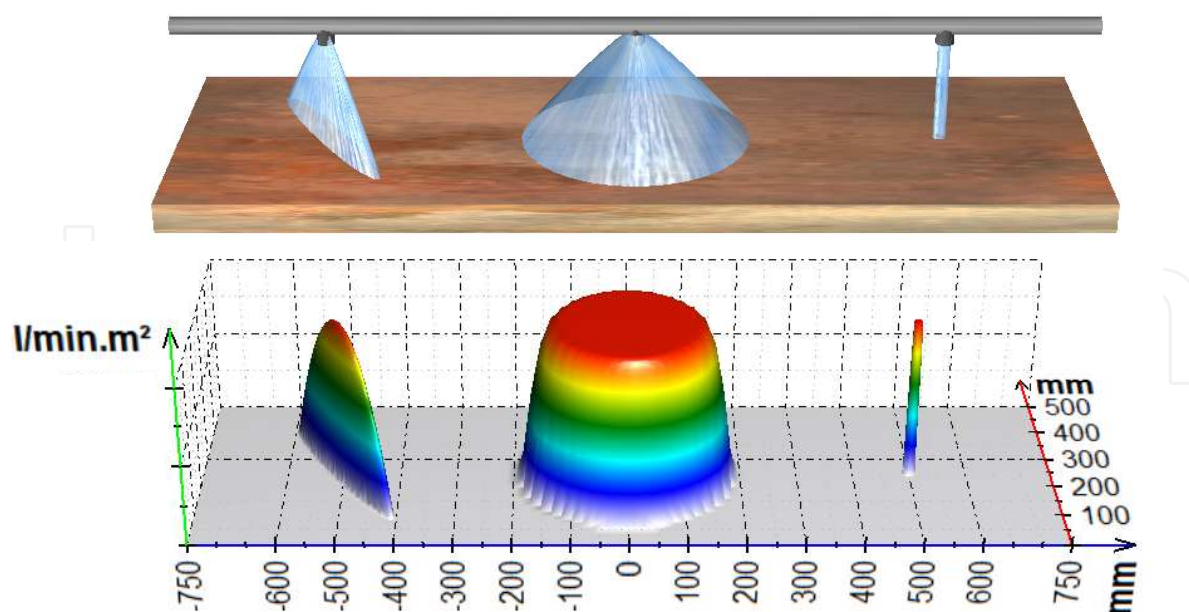
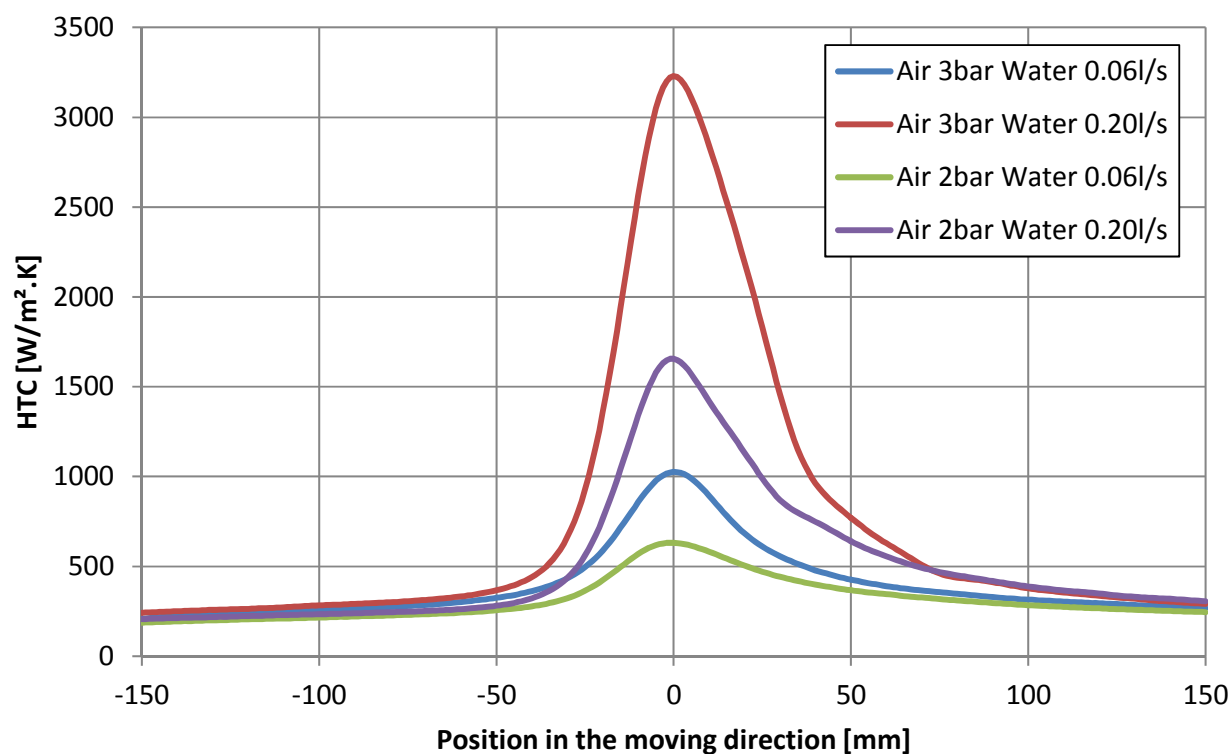**Figure 2.** Flat-jet, full-cone, and solid-jet nozzles with computed water distribution on flat surface

Figure 3. Controllability of water-air mist nozzle for surface temperatures 1000 °C

2.3. Influence of product velocity on heat transfer coefficient

Three measurements are compared when the only different parameter is the casting speed. The first experiment was stationary with no movement, the second experiment used a velocity of 2 m/s and the last experiment was done for a velocity of 5 m/s. These three experiments used the identical water-air mist nozzle, and the same pressure settings were
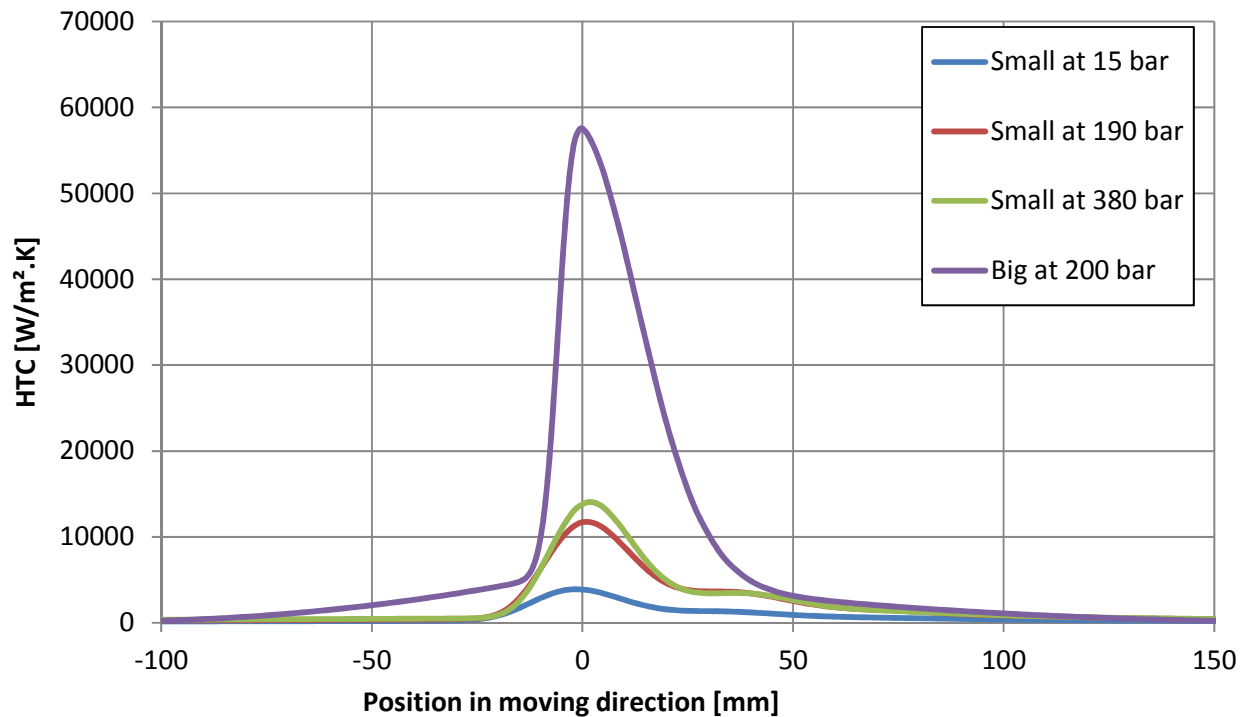
Figure 4. Distribution of HTC under spray for high pressure flat-jet nozzles for surface temperature 1000 °C.

used in all experiments - water pressure of 2 bar, air pressure of 2 bar. Fig. 5 shows the distribution of heat transfer coefficient in experimental group with a variation of velocity. HTC for the stationary case (not possible in mill) is symmetrical and the peak is narrow. The cooling intensity decreases with the increasing velocity. Heat transfer coefficient distribution is more non-symmetrical when product speed increases. The observed effect is caused by the flow on the surface and different vapor forming conditions in front and behind the impinging jet.

3. Cooling intensity and numerical models

In order to design a cooling section, knowledge of the cooling intensity is required for a group of nozzles and nozzle headers. Exact knowledge of the heat transfer coefficient as a function of spray parameters and surface temperature is the key problem for any design work. The cooling intensity is a function of several parameters, mainly, nozzle types, chosen pressures and flow rates, surface temperature of a material, and velocity of a material movement whilst under spray. There is no function available which describes cooling intensity using all the mentioned parameters. This is the reason why real measurement is absolutely necessary.

3.1. Experimental procedure

During the in-line heat treatment the product is moving so our testing sample should be also moving through the cooling section. Fig. 6 shows schematically a suitable experiment used for obtaining boundary conditions for a numerical simulation. The hot sample is moving at
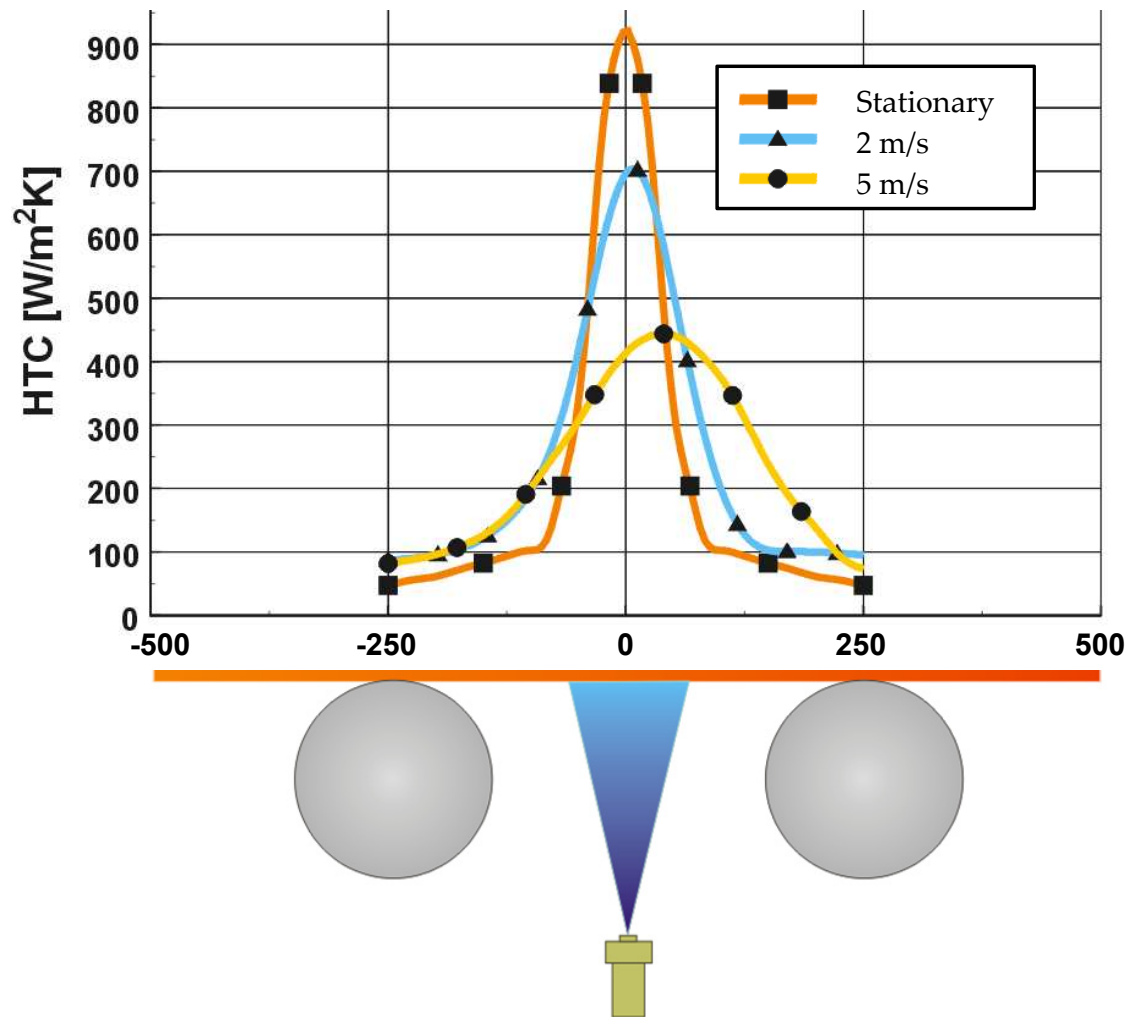
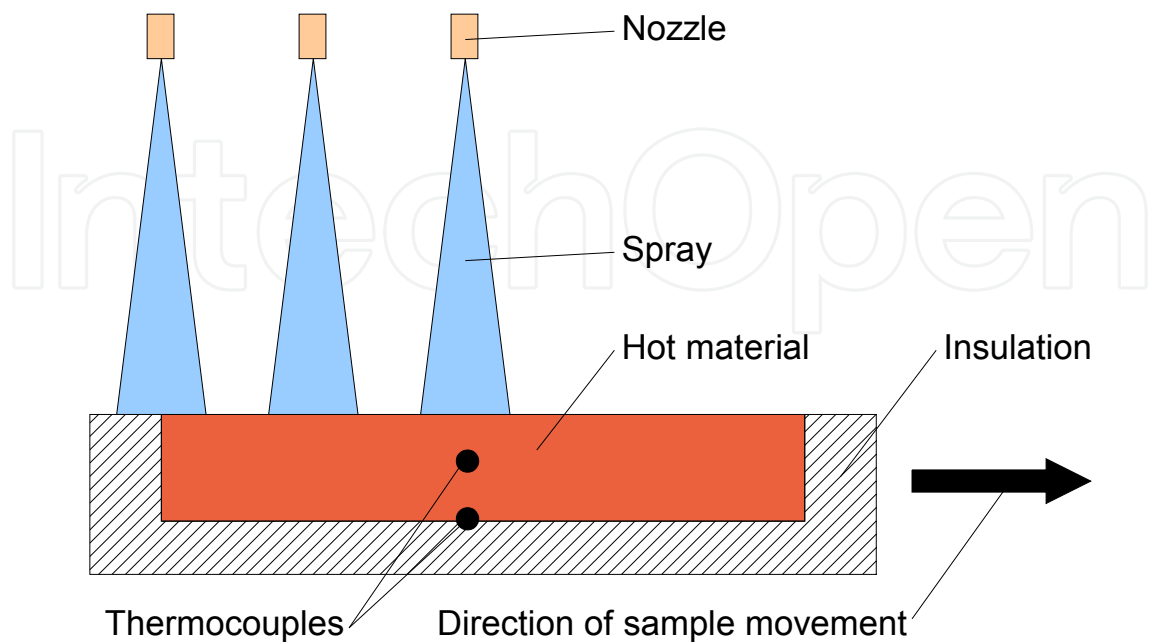**Figure 5.** Influence of velocity at heat transfer coefficient.

Figure 6. Moving sample with embedded thermocouples cooled down by water spray

prescribed velocity which is similar to real conditions. The sample passes under spray which cools down the hot sample. For a simple shape like plate it is recommended to insulate all surfaces excluding the one on which the cooling intensity is investigated. One or more thermocouples are embedded in the sample and measure temperature during the experiment. The installed thermocouples should not disturb the cooled surface. This is the reason why they should be installed inside the sample, not on the investigated surface. In principle when all surfaces are insulated except the one which is investigated one thermocouple is enough. However, this thermocouple should be as close to the investigated surface as possible. Otherwise the resolution of description of boundary conditions will be degraded. After the measurement an inverse algorithm is used to compute boundary conditions on the investigated surface from the measured temperature history inside the sample. An example of recorded temperature history is shown in Fig. 7.
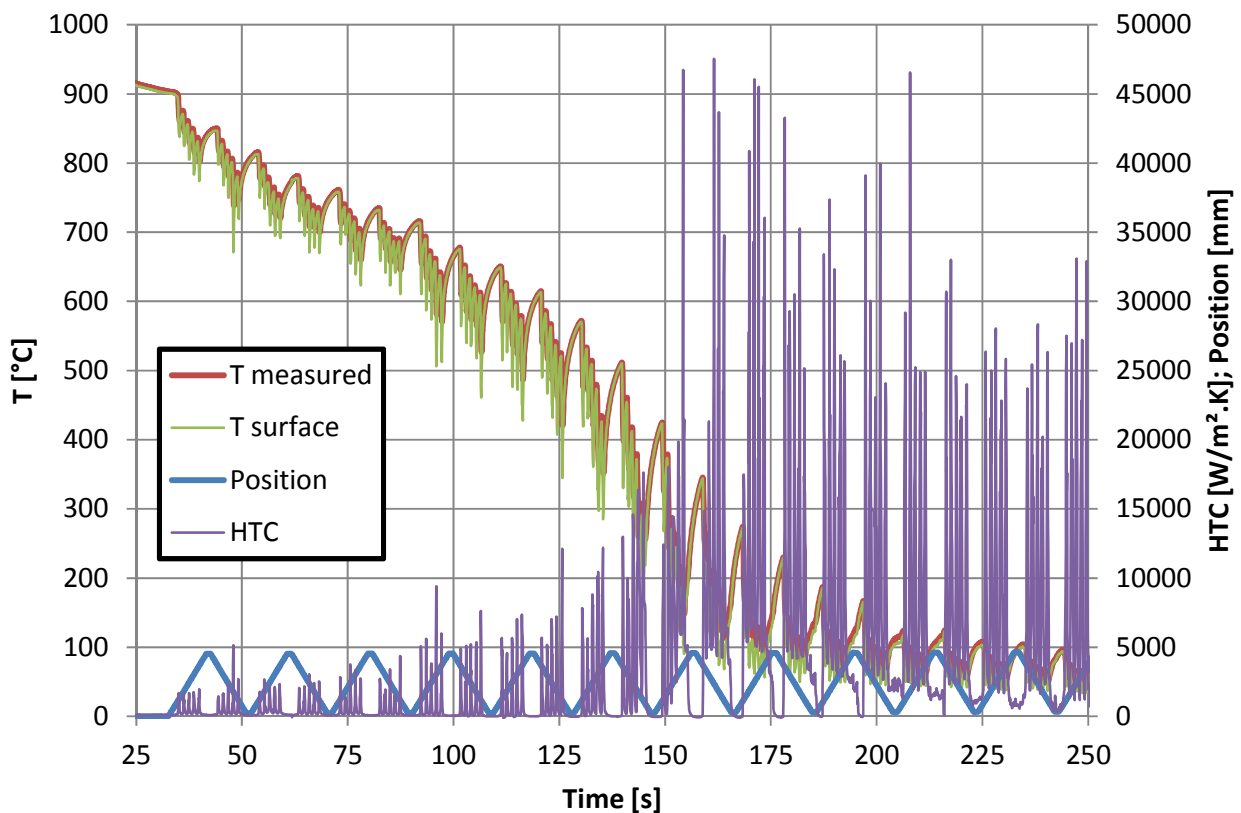

Figure 7. Example of recorded temperature history by one thermocouple inside the sample, computed surface temperature above the installed thermocouple, recorded position of the thermocouple in the cooling section, and computed heat transfer coefficient. Cooling section equipped with five rows of flat-jet nozzles.

Heat transfer test bench presented in [4] is designed so that it enables progression of samples up to the weight of 50 kg with infinitely adjustable speed from 0.1 to 6 m/s (see Fig. 7). On the supporting frame there is a carriage moving, on which the sample under examination with embedded temperature sensors and measuring system is fixed (see Fig. 9). The carriage's progression is provided by a hauling rope through a drive pulley and a motor with a gearbox. The motor is power supplied by a frequency converter with the possibility
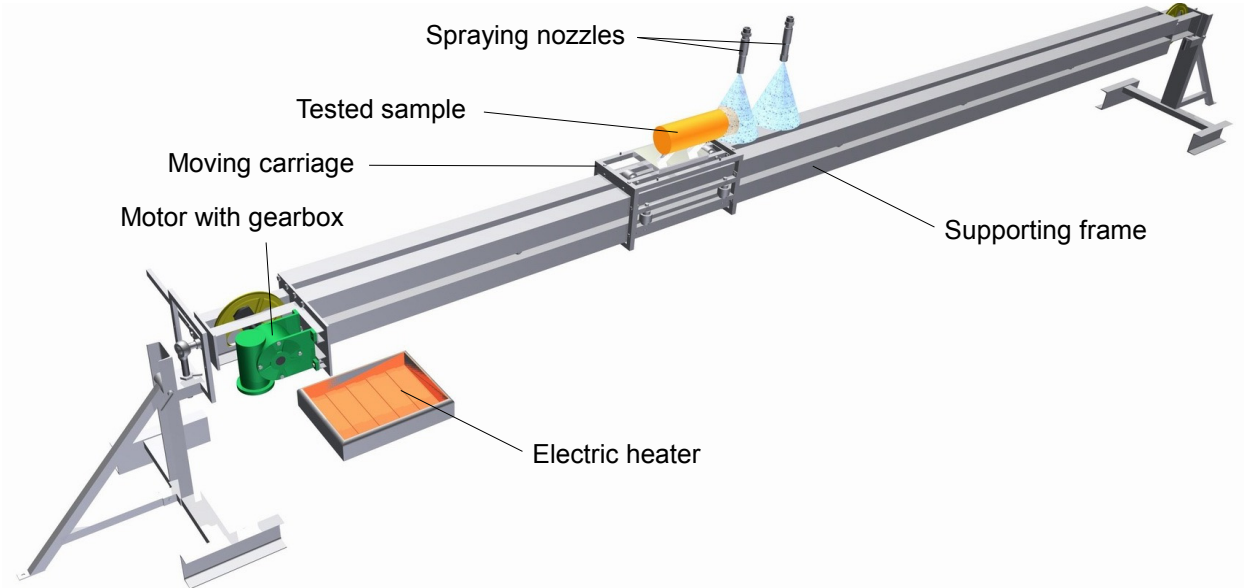
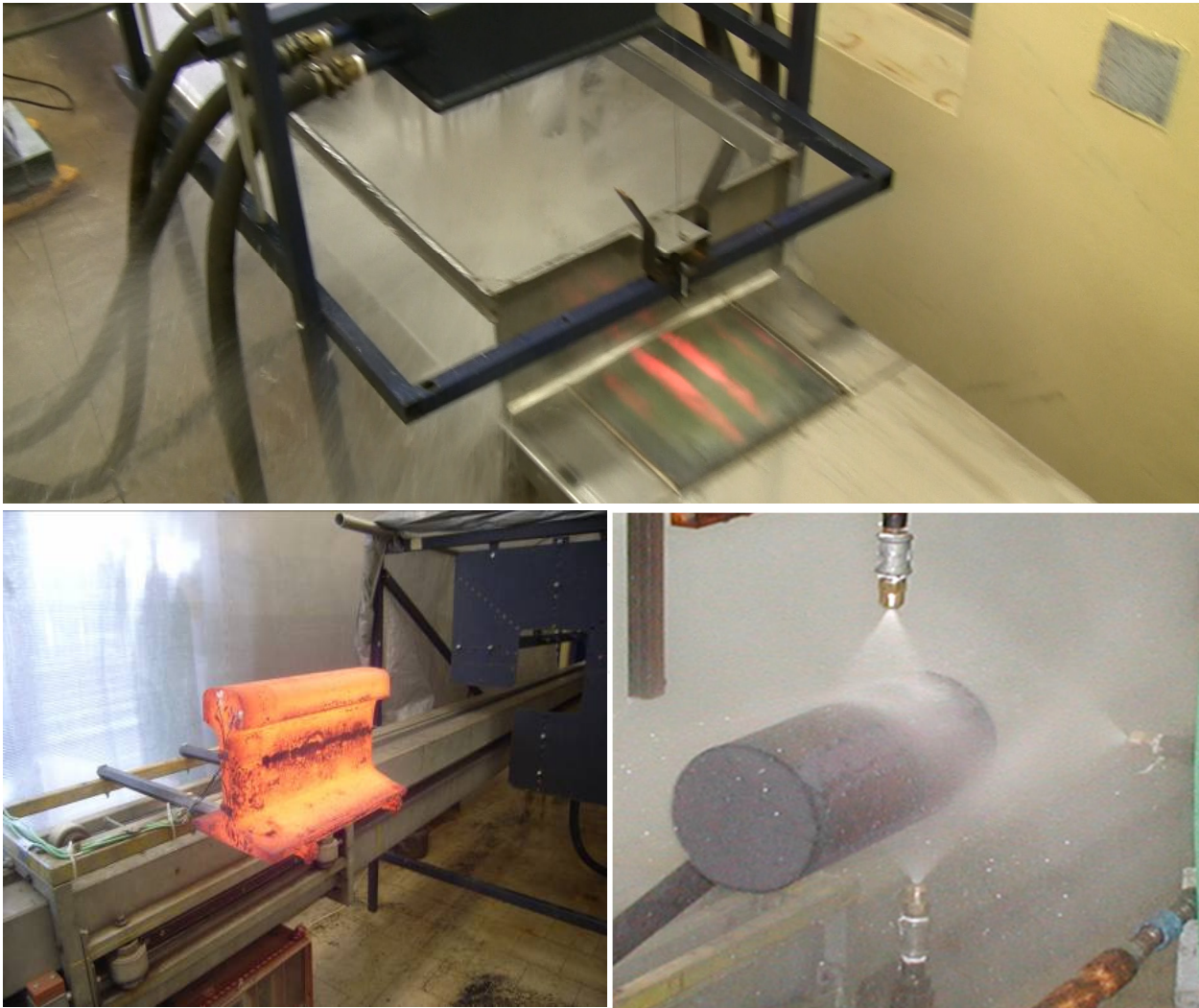**Figure 8.** Heat transfer test bench

Figure 9. Examples of boundary conditions measurements on steel plate, rail, and pipe.

of a smooth change of speed. The direction of the carriage can be reversed and passages repeated in a requiring number. The whole cycle is programmed and controlled through the superior PC. There is a spraying section in the central sector where arbitrary jets configuration can be arranged when distribution of heat transfer coefficients or heat fluxes must be measured. The sample is equipped with thermocouples connected to the data logger. The thermocouples are calibrated before use and the results of calibration are used to eliminate dynamic error in measurement of highly transient thermal processes. Before the actual experiment the carriage with the sample is positioned to the electric heater and it is heated to the required temperature inside the furnace. After the temperature in the sample is stabilized, the heating device is removed, the stand is turned to spraying position, the pump for the water gets going and the carriage's runs through the cooling section. The position of the cooled surface can be horizontal with spraying upper or bottom surfaces or vertical. Signals from the sensors are read by the data logger which moves together along with the sample. At the same time, the signal indicating the actual carriage's position is recorded as well. After performing the required number of passes through cooling zone, data are exported from data logger's internal memory into the computer for further processing.

3.2. Inverse computation of boundary conditions and numerical models

Information from temperature histories in a particular depth under the investigated surface are used as entry parameters for the thermal conduction's inverse task. Inverse task outputs are surface temperature histories, heat flows, and heat transfer coefficients (HTC) as function of time and position. Most often, in mathematical models the boundary condition of the 3'd type is used where heat flow is specified by the HTC value and the cooling water temperature.

If the boundary conditions of a solid must be determined from transient temperature measurements at one or more interior locations, it is an inverse heat conduction problem (IHCP) during which the dispersed impulse on boundary must be found. The IHCP is much more difficult to solve than the direct problem. Such problems are extremely sensitive to measurement errors. There are number of procedures that have been advanced for the solution of ill-posed problems in general. Tikhonov has introduced the regularization method [5] to reduce the sensitivity of ill-posed problems to measurement errors. The mathematical techniques for solving sets of ill-conditioned algebraic equations, called single-value decomposition techniques, can also be used for the IHCP [6]. There were extremely varied approaches to the IHCP. These included the use of Duhamel's theorem (or convolution integral) which is restricted to linear problems [7]. Numerical procedures such as finite differences [8][9][10] and finite elements [11] were also employed, due to their inherent ability to treat non-linear problems. Exact solution techniques were proposed by Burggaf [12], Imber and Khan [13], Langford [14], and others. Some techniques used Laplace transforms but these are limited to linear cases [15]. Combined approach is also described in [16]. The improvement in artificial intelligence has brought new approaches, such as genetic algorithm [17] and neural networks [18][19][20].

All the mentioned algorithms need a precise mathematical model of the tested sample for computing the direct heat conduction problem. Analytical methods may be used, in certain cases, for exact mathematical solutions of conduction problems. These solutions have been obtained for many simplified geometries and boundary conditions and are well documented in the literature [21][22][23]. However, more often than not, geometries and boundary conditions preclude such a solution. In these cases, the best alternative is the one using a numerical technique. For situations where no analytical solution is available, the numerical method can be used. Nowadays there are several methods that enable us to solve numerically the governing equations of heat transfer problems. These include: the finite difference method (FDM), finite volume method (FVM), finite element method (FEM), boundary element method (BEM), and others. For one-dimensional model with constant material properties there exists nice similarity. All of the FDM, FVM, and FEM with tent weighting function equations can be put in a similar form:

$$\frac{d}{dt}\left(\beta T_1 + \gamma T_2\right) = \frac{-\alpha}{\Delta x^2}\left(T_1 - T_2\right) + \frac{q_1(t)}{\rho c \Delta x}, \tag{1}$$

$$\frac{d}{dt}\left(\gamma T_{j-1} + 2\beta T_j + \gamma T_{j+1}\right) = \frac{-\alpha}{\Delta x^2}\left(T_j - T_{j+1}\right) + \frac{\alpha}{\Delta x^2}\left(T_{j-1} + T_j\right), \tag{2}$$

$$\frac{d}{dt}\left(\gamma T_{N-1} + \beta T_N\right) = \frac{-\alpha}{\Delta x^2}\left(T_{N-1} - T_N\right) + \frac{q_N(t)}{\rho c \Delta x}, \tag{3}$$

where β and γ have the values listed in Tab. 1. Equations (1–3) are restricted to temperature-independent thermal properties but the concepts can be extended to T-variable cases. In general for multidimensional models and temperature dependent material properties the simplest equations are obtained for FDM while the complexity of equation for FVM and FEM is several times higher.

	β	γ	$\beta + \gamma$
FDM	1/2	0	1/2
FVM	3/8	1/8	1/2
FEM	2/6	1/6	1/2

Table 1. Values of the β and γ of Eq. (1–3)

3.3. Phase change implementation

Physical processes, such as solid/liquid and solid state transformations, involve phase changes. The numerical treatment of this non‑linear phenomenon involves many problems. Methods for solving the phase change usually use a total enthalpy H, an apparent specific heat coefficient c_A, or a heat source $\dot{q}$.

The nature of a solidification phase change can take many forms. The classification is based on the matter in the phase change region. The most common cases follow:

a. *Distinct*: The phase change region consists of solid and liquid phases separated by a smooth continuous front – freezing of water or rapid solidification of pure metal.
b. *Alloy*: The phase change region has a crystalline structure consisting of grains and solid/liquid interface has a complex shape – most metal alloys.
c. *Continuous*: The liquid and solid phases are fully dispersed throughout the phase change region and there is no distinct interface between the solid and liquid phase – polymers or glasses.

In a distinct phase change, the state is characterized by the position of the interface. In such cases the class of the so called *front tracking* methods is usually used. However, in cases b) and c) the models use the phase fraction.

The phase change process can be described by a single enthalpy equation

$$\frac{\partial H}{\partial t} + \nabla \cdot \left(g_d H_d s_d + g_l H_l s_l \right) = \nabla \cdot \left(k \nabla T \right) \tag{4}$$

where g is the phase volume fraction, s is the phase velocity, and subscript d and l refer to solid and liquid phases (or structure A and structure B), respectively [24]. The k is (in this case) a mixture conductivity defined as

$$k = g_d k_d + g_l k_l \tag{5}$$

and H is the mixture enthalpy

$$H = g_s \int_{Tref}^{T} \rho_d c_d dT + g_l \int_{Tref}^{T} \rho_l c_l dT + \rho_l c_l L \tag{6}$$

where *Tref* is an arbitrary reference temperature. To overcome the problem of the non-linear (discontinuity) coefficient of a specific heat a non−linear source term is used. The term $\partial H/\partial t$ can be expanded as

$$\frac{\partial H}{\partial t} = c_{vol} \frac{\partial T}{\partial t} + \delta H \frac{\partial g_l}{\partial t} \tag{7}$$

Neglecting convection effects in Eq. (4) and substituting Eq. (7) results in

$$c_{vol} \frac{\partial T}{\partial t} = \nabla \cdot \left(k \nabla T \right) + \dot{q} \tag{8}$$

where

$$\dot{q} = -\delta H \frac{\partial g_l}{\partial t} \tag{9}$$

Eq. (4) is non−linear and it contains two related but unknown variables H and T. It is convenient to reformulate this equation in terms of a single unknown variable with

non−linear latent heat. Song [25] and [26] Comini uses so called Apparent heat capacity. The apparent specific heat can be defined as

$$c_A = \frac{dH}{dT} = c_{vol} + \delta H \frac{dg_l}{dT} \tag{10}$$

where

$$c_{vol} = g_d \rho_d c_d + g_l \rho_l c_l$$
$$\delta H = \int_{Tref}^{T} (\rho_l c_l - \rho_d c_d) dT + \rho_l L. \tag{11}$$

Neglecting convection effects and substituting into Eq. (4) yields apparent heat capacity equation

$$c_A \frac{\partial T}{\partial t} = \nabla \cdot (k \nabla T). \tag{12}$$

Another approach is total enthalpy. From Eq. (6) it can be written

$$\nabla T = \nabla H / c_{vol} - \delta H \nabla g_l / c_{vol}. \tag{13}$$

Substitution in Eq. (4) will result in a total enthalpy equation

$$\frac{\partial H}{\partial t} = \nabla \cdot \left(\frac{k}{c_{vol}} \nabla H \right) + \nabla \cdot \left(\frac{k}{c_{vol}} \delta H \nabla g_l \right). \tag{14}$$

3.4. Sequential identification inverse method

For measurements where installed thermocouple inside the investigated body disturbs also surface temperature as it is very close to investigated surface HTC must be computed directly by an inverse method. Classical and very efficient sequential estimation proposed by Beck [27], which computes heat flux instead of HTC, has several limitations. Thus new sequential identification method was developed by Pohanka to solve such inverse problems. The basic principle of time-dependent boundary conditions determination (heat flux, HTC, and surface temperature) from measured transient temperature history is based on cooling (or heating) of heated (or cold) sample with thermocouple installed inside (see Figure 6). Let us assume one-dimensional inverse problem with 3D model involving installed thermocouple for simplicity:

- Known dimensions of the sample.
- Known thermal temperature-dependent material properties of the sample.
- Known temperature profile at the beginning of the cooling (usually constant).
- All surfaces are insulated except the cooled one.
- HTC is not dependent on position.

The sample is heated before starting the measurement. Cooling is applied on one surface and temperature response inside the sample is recorded. Time-dependent boundary conditions are computed using inverse technique from the measured temperature history (see Fig. 7). Cooling of more surfaces can also be investigated when more thermocouples is used.

This new proposed approach computes step by step (time step) heat transfer coefficients (HTC) on the investigated surface using measured temperature history inside the cooled or heated solid body. However, this method can be very easily changed to compute any kind of boundary conditions, e. g. heat flux. The method uses sequential estimation of the time varying boundary conditions and uses future time steps data to stabilize the ill-posed inverse problem [28]. To determine the unknown surface HTC at the current time t_m, the measured temperature responses T_m^* are compared with the computed temperature T_m from the forward solver using n future times steps

$$SSE = \sum_{i=m+1}^{m+n} \left(T_i^* - T_i \right)^2 . \tag{15}$$

Any forward solver can be used e. g. finite volume method described by Patankar [29]. The computational model should include drilled hole, whole internal structure of the embedded thermocouple, and temperature dependent material properties.

At time zero homogeneous temperature is in the sample and thereby zero heat flux and thereby zero HTC on all surfaces is assumed. Otherwise there cannot be homogeneous temperature. This can be done e. g. by heating in furnace after enough long time. If the initial temperature is not homogeneous some modification of the algorithm is necessary for the first time step.

The algorithm starts at time index zero when the HTC is equal to zero (see Fig. 10). The algorithm uses forward solver and it computes temperature response at thermocouple position for linearly changing (increasing or decreasing) HTC (see HTC1 and T1 computed in Fig. 10) over few time steps. These time steps are called future time steps n and five of them are used in Fig. 10–Fig. 11. Determination of minimum number of necessary future time steps to stabilize sequential algorithm is described in [28]. The computed and measured temperatures histories are compared using Eq. (15) the same one as for sequential Beck approach. The slope of linearly changing HTC defined as

$$v = \frac{\partial h}{\partial t} \tag{16}$$

should be changed until the minimum of SSE function in Eq. (15) is found. Such a minimum says that the computed temperature history matches the measured temperature history the best for used linearly changing HTC during n future time steps.

When the best slope of HTC is found the forward solver is used to compute temperature field in the next time step using the computed boundary conditions. The algorithm is repeated for next time steps until the end of recorded temperature history is reached (see Fig. 11). For k
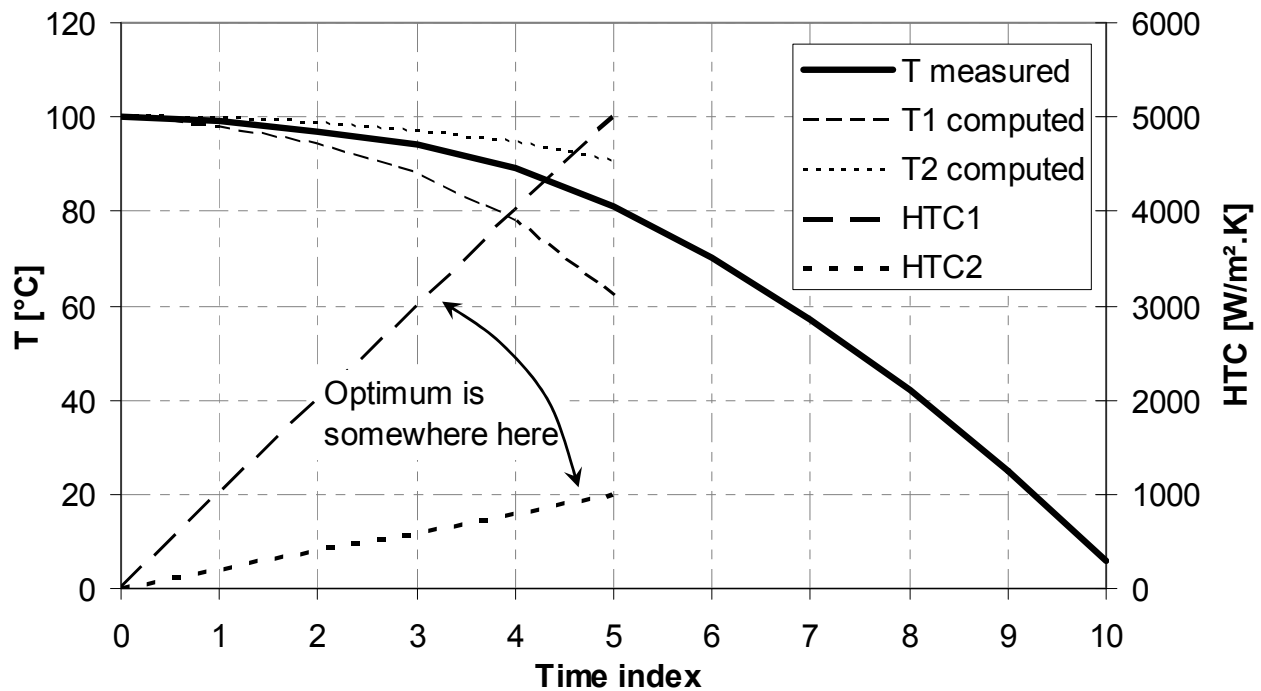
Figure 10. Measured temperature history and two computed temperature histories using two different slopes of HTC for *n* future time steps.
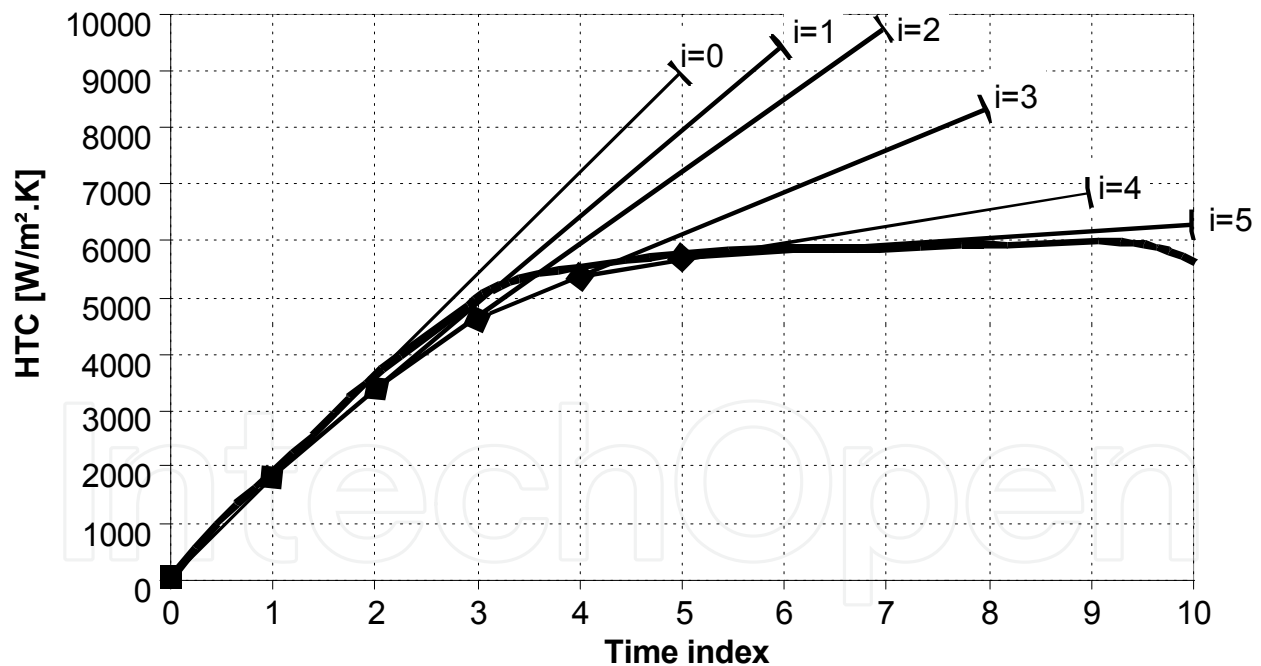

Figure 11. Real HTC and six optimum linearly changing HTC.

measured time steps only $k - n$ time steps can be computed owing to the use of future data. This method works perfectly when real HTC is almost linear in time. When the slope is abruptly changing the computed HTC curve is slightly smoother than the real one; the more future time steps are used the smoother is the computed curve of HTC (bigger difference between computed and real HTC) but the sequential identification inverse algorithm is more stable.

The SSE function described by Eq. (15) has only one minimum and is dependent only on one variable – slope of HTC (see Eq. 16). Even more the function is very close to parabolic function near the searched minimum because it is sum of square of temperature differences. Brent's optimization method [30], which uses inverse parabolic interpolation, is perfect candidate for finding the minimum of the SSE function in Eq. (15).

Brent's optimization method is based on parabolic interpolation and golden section. The searched minimum must be between two given points 1 and 2 (see Fig. 12). Convergence to a minimum is gained by inverse parabolic interpolation. Function values of the SSE function are computed only in few points. A parabola (dashed line) is drawn through the three original points 1, 3, 2 on the SSE function (solid line). The function is evaluated at the parabola's minimum, 4, which replaces point 1. A new parabola (dotted line) is drawn through points 3, 4, 2. The algorithm is repeated until the minimum with desired accuracy is found. If the three points are collinear the golden section [30] is used instead of parabolic interpolation.
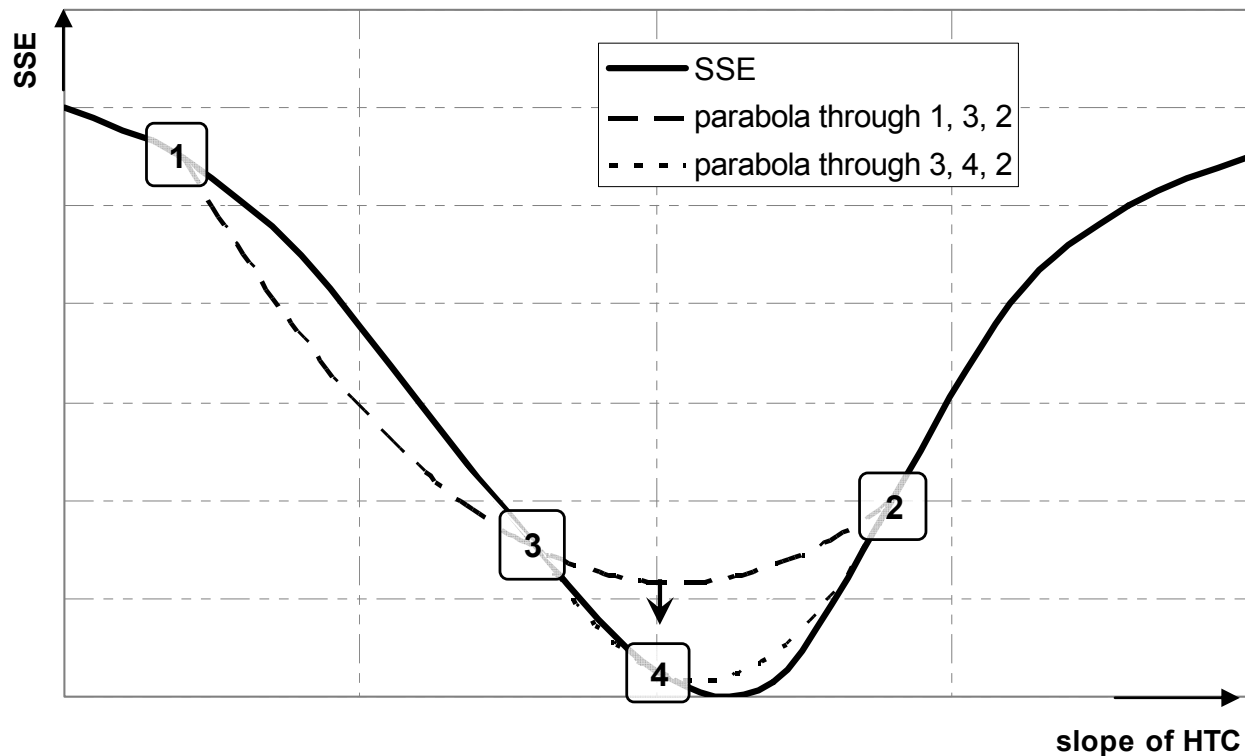

Figure 12. Convergence to a minimum by inverse parabolic interpolation.

3.5. Evaluation of boundary conditions

To demonstrate the procedure a real measurement is used. The cooling section consists of five rows of flat-jet nozzles. The heated sample passes repeatedly under the spraying nozzles. Several thermocouples in one row, which is perpendicular to the sample movement direction, were installed in the sample to be able to investigate also the cooling homogeneity across the sample. For simplicity we focus now on only one thermocouple, however, it is easy

to do the procedure for all thermocouples. Temperature record from such measurement is shown in Figure 7. Recorded position (zigzag line) of the thermocouple is shown as well and demonstrates the repeated passes through cooling section. Using the inverse method boundary conditions were computed: surface temperature and HTC. All the shown lines are function of time; however, for numerical simulation we need HTC as function of position and surface temperature. We start with surface temperature from the measurement. See Figure 13 with shown surface temperature drawn using green line as function of position. The green lines represents surface temperatures through which the plate pass during experiment. In the place where the green line is shown we also know HTC from the measurement. HTC values are shown using the color scale. HTC values between green lines are interpolated. This chart shows HTC distribution as a function of surface temperature and position and is the key point for accurate numerical simulation. HTC values above the most top green line are extrapolated and are not accurate as there are no data available from measurement. We should avoid usage of these values during numerical simulation.
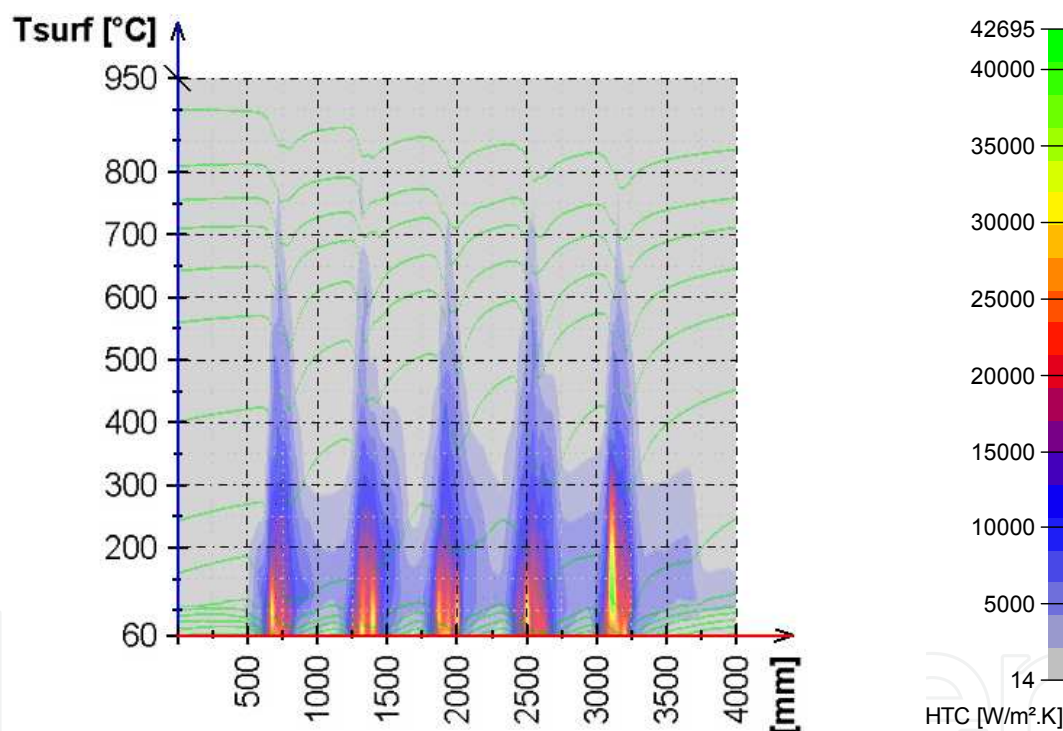

Figure 13. Prepared boundary conditions for numerical simulation from measurement shown in Fig. 7. Chart shows HTC as function dependent on position in cooling section in the direction of sample movement and on surface temperature of the cooled sample.

3.6. Numerical simulation

Having prepared boundary conditions we can do numerical simulation of cooling of products of various material properties and of various thicknesses. By repeating the boundary conditions we can simulate long cooling section with more rows of cooling nozzles. An example of such simulation is shown in Fig. 14 and is drawn in CCT. You can see computed temperature at the surface and at the center of the material. It is obvious that

the cooling rate for the surface temperature is higher than in the center. The results are drawn in CCT diagram, however, you should not that the cooling rate is far away from constant. This is very important because the CCT diagram is only informative and the final structure has to be verified by experimental measurement. There are three major reasons why cooling rate is not constant. One is caused by passing product under separate row of nozzles. The passes are obvious from T surface curve in Fig. 14. You can see drops of temperature when the product is passing under spray followed by reheating due to the internal capacity of the heat in the product. The second reason is mentioned Leidenfrost point. You can see low cooling rate in the center up to 20 s as the surface temperature is above Leidenfrost point and after that cooling rate is increasing and reaching maximum which is almost triple in comparison to value above Leidenfrost point. Decreasing of cooling rate is followed as the surface temperature is getting closer to the temperature of water. The third reason is low diffusivity for big products. The product cannot be cooled down at the same cooling rate on the surface as in the center. The lower is the diffusivity and the bigger is the product the bigger difference is between the cooling rate on the surface and in the center.
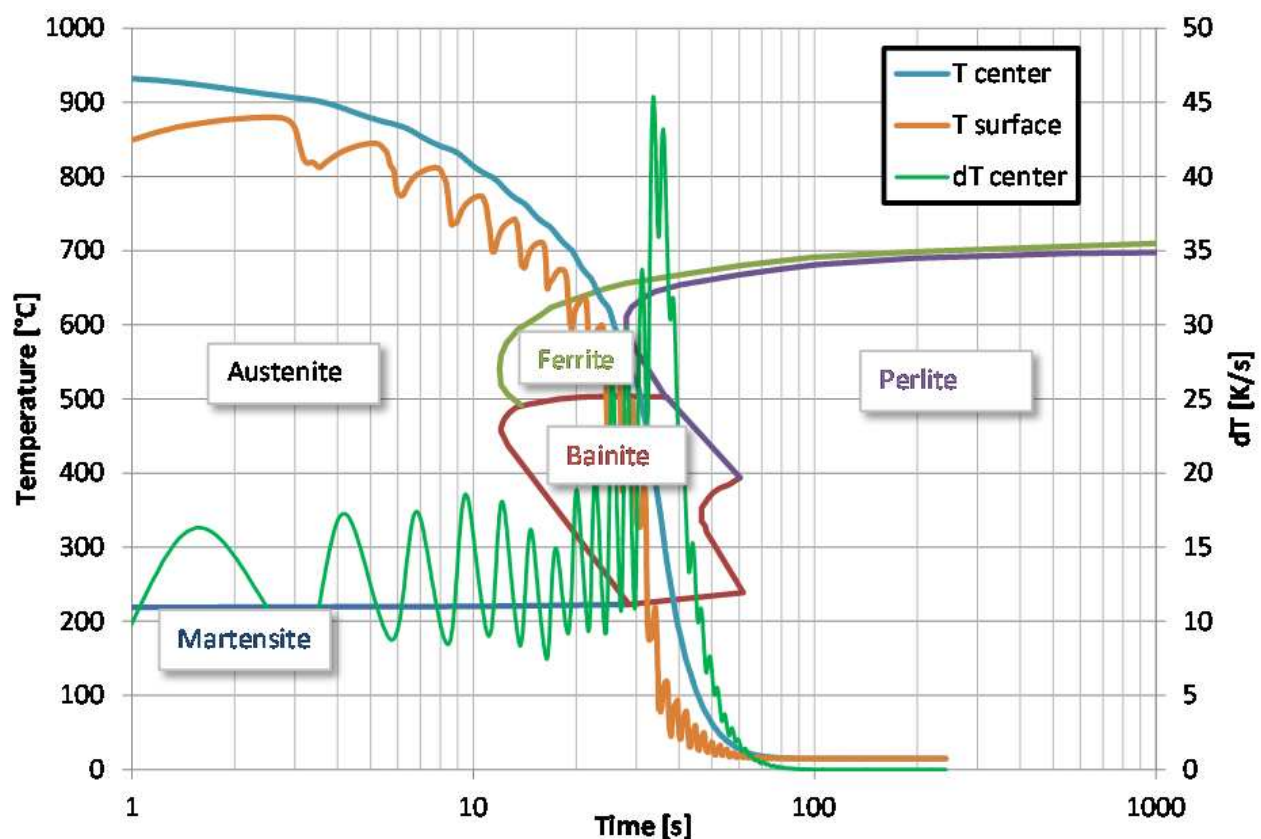

Figure 14. Simulation of cooling in the CCT diagram.

4. Verification conducted at pilot test bench

It is important to understand that cooling rate in cooling section in industrial application is far away from constant value using which CCT diagrams are obtained. Verification

functionality of a newly designed cooling system prior to its plant implementation is essential. The design obtained by using the numerical model must be verified and fine-tuned by further full-scale cooling tests. Pieces of tube, rail, wire or plate of real dimensions with implemented thermocouples are tested in the designed cooling section. The length of a laboratory test bench shown in Fig. 8 and Fig. 9 is limited, hence the sample must be accelerated prior entering the cooling section, to a velocity normally used in a plant, and after pass through cooling section, the direction of movement is reversed. In this way, the sample moves several times under the cooling sections. This cooling process is controlled by computer to simulate running under the long cooling section used normally in the plant. Nozzles, pressures, and header configurations are tested. The design of the cooling and the pressures used are modified until the demanded temperature regime and final structure is obtained. The full-scale material samples are then cut for the tests of material properties and structure.

When heat treatment is performed on larger product such as rail, mainly its head, it is not possible to achieve same cooling rate at surface and in the center of rail head. The cooling rate near surface are much faster and even more reheating can appear and can cause very different material properties (see Fig. 15). As the rail head passed under the spray the surface temperature dropped fast and was followed by reheating due to the heat stored inside the head. The reheating caused lower hardness near the surface as shown in Fig. 14. The center of the head is harder because no reheating occurred in the bigger depth. To avoid this problem the cooling section should be modified. One solution is to use more row of nozzles with smaller row pitch and also nozzles with lower HTC. This can be achieved by smaller pressure or smaller nozzles. Also replacement of flat-jet nozzle by full-cone nozzles can be considered. The Leidenfrost temperature should be also considered. We should be above Leidenfrost temperature or below but definitely not near to avoid big different cooling rates for small changes in surface temperature.
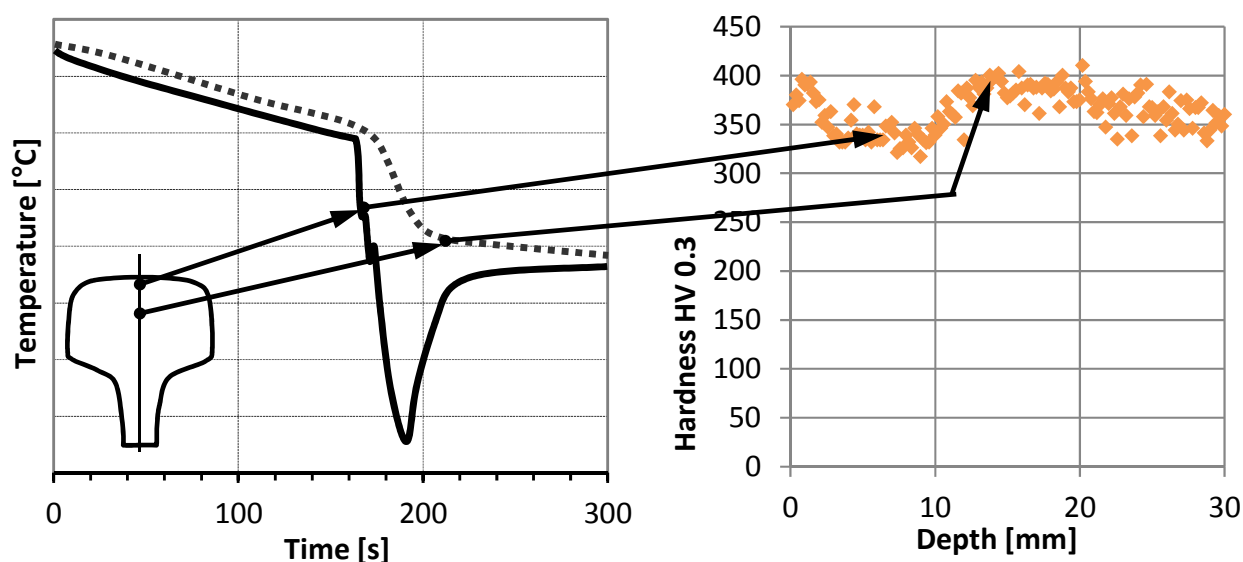

Figure 15. Measured temperature histories in a rail head in two depths and measured micro-hardness in rail head after heat treatment.

5. Concluding remarks

The design of cooling sections used for in-line heat treatment for hot rolling plants is very extensive work. It utilizes laboratory measurement, numerical modeling, inverse computations, and also pilot mill tests. The first step is the search of the best cooling regime for steels for which this is not yet known. The second step is to obtain a selection of technical means in order to guarantee obtaining the prescribed cooling rates. Nozzle configurations and cooling parameters are selected and controllability of the cooling section is checked. The final step of the design is a laboratory test using a full size sample simulating plant cooling.

Design based on laboratory measurement therefore minimizes the amount of expensive experimentation performed directly on the plant. Elimination of potential errors and enabling adjustment of control models in the plant is possible after the cooling process is tested in laboratory conditions.

Author details

Michal Pohanka and Petr Kotrbáček
Brno University of Technology, Heat transfer and Fluid Flow Laboratory, Brno, Czech Republic

6. References

[1] Raudenský, M.; Horský, J.; Hajduk, D.; Čecho, L. Interstand Cooling - Design, Control and Experience. *Journal of Metallurgical and Mining Industry*, 2010, No. 2, Vol. 3, pp. 193-202.

[2] Hnízdil, M.; Raudenský, M.; Horký, J.; Kotrbáček P.; Pohanka M. In-Line Heat Treatment and Hot Rolling. *In proc. AMPT 2010*, Paris, France, October 2010, pp. 563-568.

[3] Horký, J.; Raudenský, M.; Kotrbáček, P. Experimental study of long product cooling in hot rolling. *Journal of Materials Processing Technology*, August 1998, Vol. 80-81, pp. 337-340.

[4] Pohanka, M.; Bellerová, H.; Raudenský, M.; Experimental Technique for Heat Transfer Measurements on Fast Moving Sprayed Surfaces. *Journal of ASTM International*, Sept. 2010, Vol. 1523, pp. 3-15.

[5] Tikhonov, A. N.; Arsenin, V. Y. *Solution of Ill-Posed Problems*. Washington, D.C.: Winston, 1977. ISBN 0470991240.

[6] Mandrel, J. Use of the singular value decomposition in regression analysis. *Am. Stat.*, 1982, Vol. 36, pp. 15-24.

[7] Stloz, G. Jr. Numerical solutions to an inverse problem of heat conduction for simple shapes. *Int. J. Heat Transfer*, 1960, Vol. 82, pp. 20-26.

[8] Smith, G. D. *Numerical solution of partial differential equations*. UK: Oxford University Press, 1978. ISBN 0-198-59650-2.

[9] Beck, J. V. Nonlinear estimation applied to the nonlinear heat conduction problem. *Int. J. Heat and Mass Transfer*, 1970, Vol. 13, pp. 703-716.

[10] Beck. J. V.; Litkouhi, B.; St. Clair, C. R. Jr. Efficient sequential solution of the nonlinear inverse heat conduction problem. *J. Numerical Heat Transfer*, 1982, Vol. 5, pp. 275-286.

[11] Bass, B. R. Applications of the finite element to the inverse heat conduction problem using Beck's second method. *J. Eng. Ind.*, 1980, Vol. 102, pp. 168-176.

[12] Burggraf, O. R. An exact solution of the inverse problem in heat conduction theory and applications. *Int. J. Heat Transfer*, 1964, Vol. 86C, pp. 373-382.

[13] Imber, M.; Khan, J. Prediction of transient temperature distributions with embedded thermocouples. *Al AA J.*, 1972, Vol. 10, pp. 784-789.

[14] Lengford, D. New analytic solutions of the one-dimensional heat equation for temperature and heat flow rate both prescribed at the same fixed boundary (with applications to the phase change problem). *Q. Appl. Math.*, 1967, Vol. 24, pp. 315-322.

[15] Grysa, K.; Cialkowski, M. J.; Kaminski, H. An inverse temperature filed problem of the theory of thermal stresses. *Nucl. Eng. Des.*, 1981, Vol. 64, pp. 169-184.

[16] Sláma, L.; Raudenský, M.; Horský, J.; Březina, T.; Krejsa, J. *Evaluation of quenching test of rotating roll with unknown time constant of sensor using genetic algorithm.* Int. Conf. Mendel, Brno, 1996.

[17] Raudenský, M.; Pohanka, M.; Horský, J. Combined inverse heat conduction method for highly transient processes. In *Advanced computational methods in heat transfer VII*, Halkidiki: WIT Press, 2002, pp. 35–42. ISBN 1-85312-9062.

[18] Dumek, V.; Grove, T.; Raudenský, M.; Krejsa, J. Novel approaches to the IHCP: Neural networks. In *Int. symposium on inverse problems - Inverse problems in Engineering Mechanics*, Paris, 1994, pp. 411-416.

[19] Krejsa, J.; Sláma, L.; Horský, J.; Raudenský, M.; Pátiková, B. The comparison of traditional and non-classical methods solving the inverse heat conduction problem. In *Int. Conf. Advanced Computational Methods in Heat Transfer*, Udine, July 1996, pp. 451-460.

[20] Pohanka, M.; Raudenský, M.; Horský, J. Attainment of more precise parameters of a mathematical model for cooling flat and cylindrical hot surfaces by nozzles. In *Advanced computational methods in heat transfer VI*. Madrid: WIT Press, 2000, pp. 627‑635. ISBN 1-85312-818-X.

[21] Incropera, F. P.; DeWitt, D. P. *Fundamentals of Heat and Mass Transfer*. 4th ed. New York: Wiley, 1996. ISBN 0-471-30460-3.

[22] Kakac, S.; Yener, Y. *Heat Conduction*. New York: Hemisphere Publishing, 1985.

[23] Poulikakos, D. *Conduction Heat Transfer*. Englewood Cliffs, NJ: Prentice-Hall, 1994.

[24] Voller, V. R.; Swaminathan, C. R. Fixed grid techniques for phase change problems: A review. *Int. J. for Numerical Methods in Engineering*, 1990, Vol. 30, pp. 875-898.

[25] Song, R.; Dhatt, G.; Cheikh, A. B. Thermo-mechanical finite element model of casting systems. *Int. J. for Numerical Methods in Engineering*, 1990, Vol. 30, pp. 579-599.

[26] Comini, G.; Giudice, S. D.; Saro, O. A conservative alghorithm for multidimensional conduction phase change. *Int. J. for Numerical Methods in Engineering*, 1990, Vol. 30, pp. 697-709.

[27] Beck, J. V.; Blackwell, B.; Charles, R. C. Inverse Heat Conduction: *Ill-posed Problems*. New York: Wiley, 1985. ISBN 0-471-08319-4.

[28] Pohanka, M. Limitation of thermal inverse algorithm and boundary conditions reconstruction for very fast changes on boundary. In *Engineering mechanics 2007*. Svratka (Czech Republic), 2007, pp. 229–230. ISBN 978-80-87012-06-2.

[29] Patankar, S. V. *Numerical Heat Transfer and Fluid Flow*. Hemisphere Publishing Corporation, 1980. ISBN 0-891-16522-3.

[30] William, H. P.; Saul A. T.; William, T. V.; Brian, P. F. *Numerical Recipes in C*. 2nd ed. 1997. ISBN 0-521-43108-5.